A novel plant lectin, NTL-125, interferes with SARS-CoV-2 interaction with hACE2

Anindya Sarkar [a,1], Sathi Paul [a,1], Charandeep Singh [c,1], Nilkanta Chowdhury [d,1], Papri Nag [a,1], Swarnava Das [a], Sahil Kumar [c], Anshul Sharma [c], Deepjyoti Kumar Das [c], Dipak Dutta [c], Krishan Gopal Thakur [c], Angshuman Bagchi [d], Surbhi Shriti [a], Kali P. Das [b], Rajesh P. Ringe [c,*], Sampa Das [a,*]

[a] *Division of Plant Biology, Bose Institute, P/12 C.I.T. Scheme VII(M), Kolkata, 700054, India*
[b] *Formerly, Department of Chemistry, Bose Institute, 93/1 A.P.C. Road, Kolkata, 700009, India*
[c] *CSIR-Institute of Microbial Technology, Sector 39A, Chandigarh, India*
[d] *Department of Biochemistry and Biophysics, University of Kalyani, Kalyani, 741235, India*

A R T I C L E   I N F O

A B S T R A C T

COVID-19 caused by SARS-CoV-2 virus has had profound impact on the world in the past two years. Intense research is going on to find effective drugs to combat the disease. Over the past year several vaccines were approved for immunization. But SARS-CoV-2 being an RNA virus is continuously mutating to generate new variants, some of which develop features of immune escape. This raised serious doubts over the long-term efficacy of the vaccines. We have identified a unique mannose binding plant lectin from *Narcissus tazetta* bulb, NTL-125, which effectively inhibits SARS-CoV-2 replication in Vero-E6 cell line. *In silico* docking studies revealed that NTL-125 has strong affinity to viral Spike RBD protein, preventing it from attaching to hACE2 receptor, the gateway to cellular entry. Binding analyses revealed that all the mutant variants of Spike protein also have stronger affinity for NTL-125 than hACE2. The unique α-helical tail of NTL-125 plays most important role in binding to RBD of Spike. NTL-125 also interacts effectively with some glycan moieties of S-protein in addition to amino acid residues adding to the binding strength. Thus, NTL-125 is a highly potential antiviral compound of natural origin against SARS-CoV-2 and may serve as an important therapeutic for management of COVID-19.

Introduction

COVID-19 caused by SARS-CoV-2 virus has had profound impact on the world in the past two years. In the recent past similar group of viruses, Severe Acute Respiratory Syndrome Corona Virus (SARS-CoV), Middle East Respiratory Syndrome Corona Virus (MERS-CoV) had hit some parts of the world causing 8000 and 2500 deaths, respectively, (Weiss and Leibowitz, 2011). SARS-CoV-2 has been much more widespread and dangerous and as of February 2022 as par WHO data, the total death worldwide has exceeded 6 million. SARS CoV-2 is reported to be 96% and 80% identical to Bat corona virus and to SARS-CoV, respectively (Zhou et al., 2020). After emerging in December 2019, the novel SARS-CoV-2 very fast turned into a global pandemic wreaking havoc on global life and economy. Unfortunately, very few effective drugs or therapeutic molecules have been developed so far to combat the

virus. Health services are relying on either repurposed or other supportive drugs for treating the patients. Realizing the fact that mass scale vaccination is the only viable option to fight against the pandemic, a number of pharmaceutical companies have developed different versions of vaccines based on varying mechanisms of actions (Gao et al., 2020; Peeples, 2020). Nevertheless, being an RNA virus, its natural mutagenesis rate is quite fast. In the last one and half years, several mutant strains have evolved across the globe. Some of these newly evolved strains, reported to be more contagious with multifold higher transmission rates, played havoc in some countries. Considering the continuous evolution of the mutants in a very short period of time, it is now a very valid question as to how long the present vaccines will provide protection. Currently, as a general feature of severe pandemic diseases several waves of viral attack have hit most parts of the world and, it is predicted that if we are not able to find ways to control the virus it may

likely cause much more harm.

Numerous studies have been aimed to combat this deadly virus by developing therapeutic agents which has the ability to target either the receptor of the human cells or on the virus itself. Major strategies explored in this regard involves 1) prevention of viral RNA synthesis; 2) blocking of viral enzymes to inhibit viral replication; 3) disruption of viral assembly by targeting the structural proteins of the virus; 4) blocking of the virus-host cell interaction.

Recent studies revealed that SARS-CoV-2 belonging to Coronaviridae is an enveloped virus with a positive sense large single stranded RNA genome and a nucleocapsid of helical symmetry. The 3′ terminal part of the genome contains four structural proteins, namely, the envelope protein (E), membrane protein (M), the spike glycoprotein (S) and Nucleocapsid protein (N). The S, Spike glycoprotein, interacts with human ACE2 receptor (hACE2) through its receptor-binding domain (RBD) (Lan et al., 2020). The S protein has two subunits S1 and S2 (Fig. 1A, B). S1 contains the RBD which binds to hACE2 (Yang et al., 2020; Huang et al., 2020). The junction between S1 and S2 subunits are
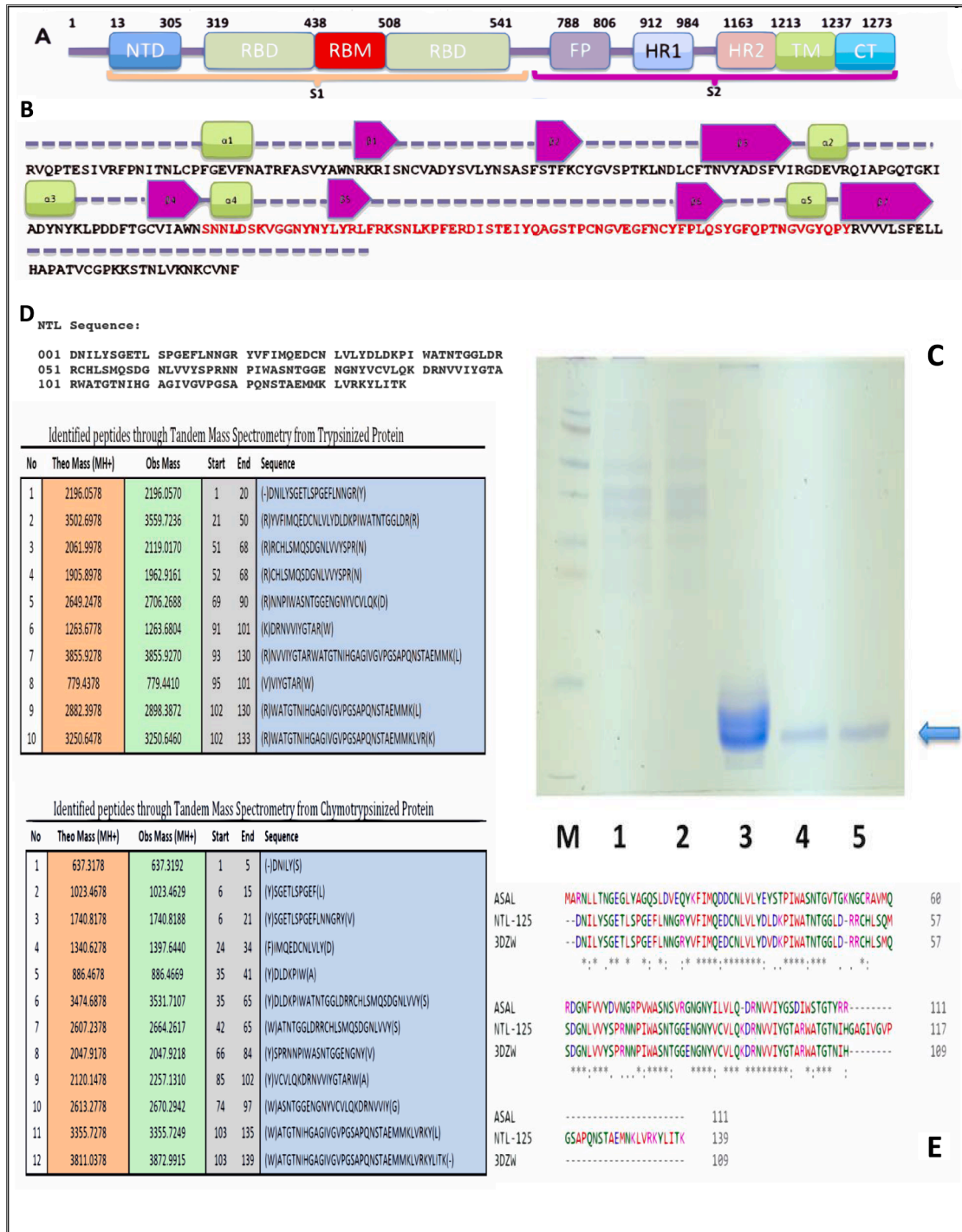
Fig. 1. Details of SARS CoV-2 Spike, NTL-125, ASAL and 3DZW proteins. (A) Schematic diagram of the spike protein showing different domains. (B) Sequence of spike RBD domain and RBM in red, with secondary structural elements. (C) Representation of lectin purification analysed in 15% SDS-PAGE, Lane M: Molecular weight marker, Lanes 1,2: semipurified proteins, Lanes 3: Purified ASAL, lanes, 4-5 NTL-125 monomer resolving at ~15kDa. (D) Identified sequence of NTL-125 from Narcissus tazetta bulb. (E) Multiple sequence alignment of ASAL, NTL-125 and 3DZW.

cleaved by host cell surface proteases, furin and transmembrane serine protease 2 (TMPRSS2) paving the path for the S2 mediated virus-host membrane fusion (Xia et al., 2020). Indeed, S protein plays the crucial role in viral pathogenesis by mediating in the virus entry into the host cell. This is why, strategies to block the binding mechanism between ACE2 and S protein has attracted so much attention of the researchers for therapeutic drug development.

Various types of agents ranging from small peptides (Ho et al., 2006; Xiang et al., 2021), chimeric proteins (Lei et al., 2020), monoclonal antibodies (Coughlin et al., 2009; Pascal; et al., 2015), and other molecules (Gurevich and Gurevich, 2014; Ngo and Garneau-Tsodikova, 2018; Xiu et al., 2020) were explored for this purpose. Researchers also start investigating the repurposing of medicines used for other ailments for treating COVID-19 (Ho et al., 2007; Kadam and Wilson, 2017; David et al., 2021).Anti-influenza drug Arbidol and anti- HIV drug, Lopinavir were tried with, but severe gastronomical adverse effects were found when lopinavir and ritonavir were tested against SARS-CoV-2 infected patients (Cai et al., 2020). Recently, in some countries Remdesivir, originally intended for the treatment of Ebola was also found to have some inhibitory effect on corona virus (Caley et al., 2020). But the medical advisory boards in many countries have recommended for limited use of this drug for hospitalized adult. All the above repurposed drugs have limited success in treating COVID-19. Entry inhibitors for SARS-CoV-2 may become more effective drugs for treating SARS-CoV-2, considering the limited success of current therapies for COVID-19.

Interestingly, towards the end of last century, lectins from plants, mushrooms and other sources were found to inhibit several viral diseases. HIV replication was shown to be inhibited by lectins (Balzrini et al.,1992; Balzarini et al., 2005; Kachko et al., 2013; Keefe et al., 2011). Lectins antagonized replication of different corona viruses including SARS-CoV (Kumaki et al., 2011). A carbohydrate-binding protein from the edible beans effectively blocks the infections of influenza viruses and SARS-CoV-2 (Liu et al., 2020). Also a few others too have anti-influenza activity (Song et al., 2007; Kim et al., 2018). In this respect different investigators demonstrated strong inhibitory effects of different species of *Narcissus* lectin against several viruses including respiratory syncytial virus, influenza A (H1N1, H3N2, H5N1) and B viruses (Kaku et al., 1990; Sauerborn et al., 1999; Balzarini, 2006; Ooi et al., 2010). The present investigating group has previous experiences with few mannose binding monocot lectins having antagonistic effects against a number of phloem sap- sucking insects (Gatehouse et al., 1995; Datta et al., 2005a; Datta et al., 2005b; Saha et al., 2006a; Chakraborty et al., 2009; Roy et al., 2014) and plant viruses vectored by sap-sucking insects (Banerjee et al., 2004; Saha et al., 2006b; Das et al., 2021). Due to these striking inhibitory features of some members of the monocot mannose binding lectin super family against varied pathogens (Zhou et al., 2010; Mitchell et al., 2017; Nascimento et al., 2021), we got interested in investigating the efficacies of a well characterized mannose binding dimeric lectin, *Allium sativum* leaf agglutinin (ASAL) (Bandyopadhyay et al., 2001) and another newly identified tetrameric, *Narcissus tazetta* lectin (NTL-125) against transmission and spread of infection of SARS CoV-2. This study offers a new insight on the role of the naturally occurring biological molecules as a potentially effective therapeutic agent against SARS-CoV-2.

Materials and methods

Materials

Narcissus tazetta (Daffodil) bulbs were collected from plants grown in departmental glass house of Bose Institute, India. *Allium sativum* leaves were collected from the plants grown in Madhyamgram Experimental farm of Bose Institute, India. Trypsin (Gold Trypsin, Promega,USA), α-Chymotrypin (SRL, India), Vero-E6 cells, HEK293T cells, SARS-CoV-2 virus, SARS-CoV-2 spike pseudo virus, RNA extraction kit (MDI Devices, India), DiAGSure nCOV-19 detection assay kit (GCC Biotech, India),

Profection mammalian transfection kit (Promega Inc.), DMEM (Gibco), Bright-Glo luciferase substrate (Promega Inc., USA) were used as received.

Protein purification

Fresh Daffodil bulbs were extracted thoroughly in 1X Phosphate Buffer Saline (PBS), pH 7.4 and filtered through a fine mesh cloth. One mL of Dimethyl Sulfoxide (DMSO) and 35 mg Phenyl methyl sulfonyl fluoride (PMSF) were added per litre of filtrate and kept overnight at 2-8°C. Next day, after centrifugation, the pH of the supernatant was adjusted to 9.0 and 20 mM $CaCl_2$ was added, mixed and stored at 2-8°C overnight. To the suspension $(NH_4)_2SO_4$ was added at pH 7.0 and kept at 2-8°C for 6-8 h. After centrifugation the pellet was collected and dissolved in 1X PBS buffer and subjected to Affinity chromatography using D-Mannose Agarose (M6400, Sigma, USA) column. The purified N. *tazetta* lectin (NTL-125) was eluted with 20mM Diaminopropane (pH 9.0). ASAL protein was purified from fresh garlic leaves following the method of Bandyopadhyay et al., (2001).

Hemagglutination assay

Purified NTL-125 protein was dispensed into different wells of microtitre plate at varying amount of 1–10 μg. Separately, rabbit erythrocytes were recovered by centrifugation form 1 mL blood and further washed with 0.9% saline solution. Twenty microliter of erythrocyte suspension was dispensed to microtitre well and kept at 25°C. In separate set of experiments aliquots of NTL-125 were independently incubated at 25, 37, 50 and 60°C for 30 mins and dispensed to wells containing erythrocyte suspension to determine the agglutination efficacy after incubation for an hour.

Intact mass analysis

Purified NTL-125 sample was analyzed by Electrospray Ionization Mass Spectrometry (ESI-MS) (Waters Corporation, Milford MA, USA) for determining the molecular mass. Purified protein sample (10μg) taken in 1 mL of 0.1% formic acid (FA) and directly infused onto the ionization chamber of ESI-MS mass spectrometer (Waters, Xevo G2-XS QTof) in positive mode with a flow rate of 5 μL/min and Capillary voltage of 3 kV, source temperature at 120°C, sampling cone 40 V and desolvation temperature at 250°C. The nitrogen flow rate was kept at 600 to 1200 lit/hr at 100 psi. Mass spectra were acquired from 50 to 2000 m/z for 1 min. Acquired raw data was deconvoluted using MaxEnt 1 software version 4.0, Waters Corporation.

SDS-PAGE analysis

Purified NTL-125 and ASAL lectins were resolved in 15% SDS-PAGE using a mini gel electrophoresis system (Mini-Protean, Bio-Rad Laboratories) and Tris-glycine (pH 8.3) and SDS as the running buffer. After staining with Coomassie brilliant blue (CBB), followed by destaining, gel images were captured using the Gel Doc XR System (Bio-Rad)

In-gel digestion

In-gel digestion of NTL-125 was performed to determine the protein sequence. The purified protein band was excised from the gel. The CBB stain was removed from gel piece by incubating with 50% 25 mM NH_4HCO_3 and 50% (v/v) acetonitrile solution. The destained gel pieces were dehydrated with 100 % acetonitrile (ACN) for 10 min in a microcentrifuge tube followed by drying in a vacuum centrifuge. Dried gel pieces were further reduced with 10 mM DTT for 45 mins at 55°C and alkylated with 55 mm iodoacetamide for 30 mins at room temperature in dark. After removing the iodoacetamide the gel pieces were washed with 50% 25 mM NH_4HCO_3 and 50% (v/v) acetonitrile solution at room

temperature. The protein in the gel pieces was then cleaved with Trypsin (Gold Trypsin, Promega, USA) and α-Chymotrypsin (SRL, India) individually using 1:20 ratio of enzyme to substrate in 25 mM ammonium bicarbonate buffer (pH 8.0). The gel pieces with enzyme solutions were incubated on ice for 1hr. Thereafter sufficient amount of 25 mM NH_4HCO_3 was added to dip the gel pieces and incubated at 37°C overnight (Gundry *et al.*, 2009). Next day the supernatant containing the peptides was collected in a new microcentrifuge tube. Digested peptides were further extracted from the gel pieces with 50% (v/v) acetonitrile, 1% (v/v) formic acid and 49% H_2O and finally dried using vacuum centrifuge.

Liquid chromatography electrospray ionization tandem mass spectrometry

LC-ESI-MS/MS analysis of the peptides derived from in-gel digestions was performed with a Waters ACQUITY UPLC M-Class System (Waters Corporation, Milford MA, USA) equipped with Xevo® G2-XS Q-Tof MS (Waters Corporation, Milford MA, USA) via an electrospray ionization source (ESI). The dried peptides were reconstituted in 20 μL of 0.1 % formic acid. Twenty microlitre of this peptide solution was then diluted to 60 μL with 0.1 % formic acid within the instrument before being injected into the Acquity UPLC-BEH C18 column (pore size 130Å, particle size 1.7 μm, inner diameter 2.1 mm x length 100 mm) (Waters Corporation, Milford MA, USA) with a trapping time of 3 min. The mobile phase consisted of two solvents: (A) 0.1% FA in water and (B) 0.1% FA in ACN. The flow rate was kept at 30 μL/ min. The total run time of 12 min was set as follows: 0 to 2 min- equilibrium, 2 to 10 min- gradients from 0% to 90% of mobile phase B and from 90% to 0% of mobile phase A, 10 to 12 min- washing with 0.1% FA. Isocratic flow of isopropyl alcohol was used in parallel with the gradient to ensure smooth and effective elution of the peptides. The eluent from the LC column was then subjected to MS in ESI (+ve) platform at 3 kV. Data dependent acquisition was recorded using Mass Lynx Version 4.0 software (Waters Corporation).

Peptide mapping

MS/MS spectra were processed and analyzed through Protein Lynx Global Server[TM] (PLGS) version 3.0.3. Peptide identification was assigned by searching against the *Narcissus tazetta* lectin protein database. The search parameters such as peptide tolerance, fragment tolerance and mass error tolerance were kept at default. Peptide identification was restricted to tryptic and chymotryptic peptides separately with no more than one missed cleavage. Cysteine carbamidomethylation was considered as a fixed peptide modification, whereas methionine oxidation as variable peptide modification. The ion matching requirements were kept at the stringency of Fragment/Peptide -2, Fragment/Protein -5 and Peptide/Protein -1 for Chymotrypsin and Fragment/Peptide -1, Fragment/Protein -1, and Peptide/Protein -1 for Trypsin.

Cell viability assay

The cell viability assay was performed by using MTT assay reagent. Vero-E6 cells were plated at 25000/well density in 100 μL of growth medium in 96-well microtiter plates for 16-24 hours at 37°C in a humidified chamber with 5 % CO_2. Next day, 50 μL of media was removed from each well and 50 μL serially diluted lectins were added. 70 % Ethanol was used as a positive control for the induction of cytotoxicity. Each lectin was used at the concentrations of 0.5, 5, 10, 20, 50 μg/mL. The plate was incubated for 48 hours (37°C, 5 % CO_2) and 10 μL of MTT solution was added to each well. The plate was further incubated for another 4 hrs in the humidified CO_2 incubator after which 100 μL of dissolving solution (10 % SDS in 0.01 M HCl) was added to each well and incubated in CO_2 incubator overnight. Viability of cells was recorded in comparison to the untreated cells by measuring the absorbance at 570

nm.

Inhibition assay of SARS- CoV-2 genome

The SARS-CoV-2 virus stock (verified by matching with original SARS-CoV-2 genome sequence) was prepared in VeroE6 cells and viral growth was confirmed by observing cytopathic effect in the culture flasks. All the experiments including virus culture and anti-viral assays were carried out in the BSL-3 laboratory following relevant ethical and biological safety clearances by institutional committees of IMTECH, Chandigarh. The virus stock was titrated by using Vero-E6 cells to estimate plaque forming units per ml of virus suspension (pfu/mL) and stored at -80°C for further use. To monitor the efficacy of lectins on SARS-CoV-2, Vero-E6 cells were seeded in 48-well plate (4×10^4 cells/ well). The lectin at various concentrations was separately incubated with 1000 pfu of virus for 1 hour. The virus-lectin suspension was then added to the wells containing Vero-E6 cells and incubated for 48 hours at 37°C in a humidified chamber with an atmosphere of 5% CO_2. 140 μL supernatant was harvested and processed for viral RNA extraction by Manufacturing & Delivering Innovations (MDI) devices, India. The qRT-PCR was performed using 8 μL of the eluted RNA sample as a template by using DiAGSure nCOV-19 detection assay kit from GCC Biotech (India). The quantification of viral RNA (cycle threshold [Ct] profile) present in the culture supernatant was determined by analyzing qRT-PCR data. The percent (%) inhibition was calculated based on the difference in Ct values between no inhibitor control and lectin wells.

Preparation of pseudo-typed SARS- CoV-2 and pseudo-virus neutralization assay

The viral entry inhibition assay was performed by using SARS-CoV-2 spike pseudo virus harboring reporter Luciferase gene. HEK293T cells were transiently transfected with plasmid DNA pHIV-1 NL4.3Δenv-Luc and Spike-Δ19-D614G by using Profection mammalian transfection kit (Promega Inc.), incubated for 72 h. Virus culture supernatant was harvested, centrifuged for 10 min at 2000 rpm followed by filtration via 0.22 μm filters, and stored at -80°C for further use. 293T-hACE-2 (BEI resources, NIH, Catalog No. NR-52511) or Vero/TMPRSS2 (JCRB cell bank, JCRB #1818) cells expressing the human ACE2 or ACE and TMPRSS2 receptors respectively were cultured in DMEM (Gibco) supplemented with 5% FBS, penicillin-streptomycin (100 U/ml). The viral entry inhibition by lectin was assessed in both 293T-ACE-2 and Vero/TMPRSS2 cells. The lectins were serially diluted in 50 μL growth medium after which 50 μL diluted pseudovirus equivalent to 2×10^5 relative luminescence units (RLU) was added. The mixture was incubated for 1 hour after which 4×10^4 cells/well (Vero/TMPRSS2 or 293T-hACE2) were added. The plate was incubated for 48 hours in humidified incubator at 37°C with 5 % CO_2. The luminescence was measured by adding 50 μL Bright-Glo luciferase substrate (Promega Inc., USA) by using Cytation-5 multi-mode reader (BioTech Inc.) The luciferase activity detected as RLU that determined the quantification of virus infection. Percent reduction of infection was estimated with reference to SARS-CoV-2 pseudovirus infection in the absence of lectin. Pseudovirus infection inhibitory concentration (IC_{50}) was determined as the concentration at which infection was reduced by 50%.

3D Structure Building of NTL-125, ASAL and 3DZW-V36L

NTL-125: The tetrameric crystal structure of the mannose binding lectin from *Narcissus pseudonarcissus* (PDB id: 3DZW) (Sauerborn et al., 1999) was used for model building as the NTL-125 and 3DZW have 99.08% sequence identities with an E-value of 1×10^{-78}. Knowledge-based *ab-initio* modeling method was used to build 30 amino acid residue C-terminal part using Robetta (Kim et al., 2004) webserver. The full-length structure of NTL-125 was finally constructed by combining the aforementioned two parts of the NTL-125 protein using

the Build Protein Module of Discovery Studio (DS).

ASAL: Homodimeric ASAL protein sequence was obtained from GenBank accession EU252577 (Benson et al., 2012). Crystal structure of mannose-specific garlic lectin (PDB id: 1KJ1) (Ramachandraiah et al., 2002) was used as template for model building of ASAL using Build Protein Module of Discovery Studio (DS).

3DZW-V36L: Mutated version of 3DZW, where Val residue at the 36th position was substituted by Ile, was built using the Build Mutant Module of DS. The mutation V36L was incorporated into the crystal structure of 3DZW at the corresponding position.

Three built structures were subjected to energy minimization separately in GROMACS (Abraham et al., 2015) using the force-field CHARMM (Brooks et al., 1983) in presence of SPC/E (Berendsen et al., 1987) explicit water model, following the steepest descent algorithm, and then by conjugate gradient algorithm.

To verify the authenticity of the built model the amino acid sequence of NTL-125 was given as input and three models were generated using three different web servers namely, Robetta,SwissModel and Phyre 2. These Models were superimposed on each other for comparison.

Molecular Docking and Simulation

NTL-125, ASAL and 3DZW-V36L structures independently were docked blindly with the SARS CoV-2 trimeric Spike glycoprotein using the ZDock tool, followed by RDock refinement present in DS. To understand the initial step of infection, Lan et al., (2020) determined the structure of Receptor Binding Domain (RBD) of the spike (S) protein bound to the ACE2. The glycosylated spike protein structure was kindly shared with us by Dr Robert J. Woods, Dr Oliver C. Grant and Dr Lance Wells (Zhao et al., 2020). The glycosylated spike protein structural information was shown by Lan et al., (2020). The Receptor Binding Domain (RBD) of the spike (S) protein falls within 319–541 amino acids and the Receptor Binding Motif (RBM) is spanning over the 438–508 amino acids whereas the S1 spans from 13–685 and S2 from 686–1273 amino acids. The best pose was selected based on their docking ZRank scores. The fourth docking between Spike and ACE-2 proteins was done using template-based docking approach in DS and 6M0J crystal structure of ACE-2 (PDB id: 6M0J) was used as a template. After energy minimization binding free energy (ΔG) were calculated using web server (Xue et al., 2016).

In silico Mutant Interaction and Binding Free Energy Estimation

All the mutations of Spike protein as shown in Table S1 were incorporated into the built Spike-NTL-125 complex and Spike-ACE2 complex separately. Total 26 mutant complexes (thirteen mutant Spike-NTL-125 and thirteen mutant Spike-ACE2) were built which were subjected to energy minimizations using the aforementioned protocol and the binding free energy (ΔG) values were calculated.

Insilco mutations of the interacting residues of NTL-125 and its effect on binding free energy in Mutant NTL-125 and RBD complex

In order to check the role of relevant interacting residues of the NTL-125 protein, deletion of the C-terminal parts from each of the monomers from the tetrameric structure of NTL-125 was performed (C-delta-Mutant). The deletion C-delta-Mutant of NTL-125, was subjected to energy minimizations following the same protocol as mentioned before. The final energy minimized structure of the C-delta-Mutant of NTL-125 was docked onto the RBD and the binding free energy values of the interactions were checked. Another set of mutations were incorporated in the NTL-125 spanning the amino acid residues 80 to 83 applying the *insilico* alanine scanning mutagenesis to check the effects of mutations on RBD binding.

Results

Characterization of purified lectins

Purified ASAL and NTL-125 were run in 15% SDS-PAGE that showed the bands corresponding to ~ 12.5 kDa and ~ 15 kDa proteins, respectively (Fig. 1C), (arrow indicating the band of NTL-125). The purity of the proteins was validated by hemagglutination assay with rabbit erythrocyte at a temperature ranging between 25-50°C (Fig. S1). Both ASAL and NTL-125 readily agglutinated rabbit erythrocytes at room temperature but failed to show any activity when pretreated above 37°C which confirms the native structural integrity of the lectins at and below 37°C.

NTL-125 protein was analyzed through LC-MS for intact mass, peptide mapping and amino acid sequencing. The mass spectrum of NTL-125 was deconvoluted by MaxEnt 1 software. It showed an intact tetrameric mass of 61.2 kDa. Peptides were identified through tandem mass spectrometry after digestion of the protein using trypsin (Fig. S2, S3) and chymotrypsin (Fig. S4, S5). Trypsin digestion of NTL-125 produced 10 major peptides whose theoretical and observed mass values and the identified peptide sequences are shown in Fig. 1D. The sequence information was verified from the overlapping peptides generated by α-Chymotrypsin digestion (Fig.S6) that produced 12 major peptides also shown in Fig. 1D. The overlapping sequence data from the two digests were aligned to create the primary sequence of NTL-125. BLAST searching revealed strong similarity of NTL-125 to mannose binding lectin proteins from different plant sources (Fig. 1E). However, the final sequence of NTL-125 comprising 139 residues is unique primarily because of the existence of a 30 residue (110-139) C-terminal tail. This sequence was submitted to Uniprot knowledge base (accession number COHU1).

Inhibition of SARS-CoV-2 replication in cell culture by NTL-125

Both ASAL and NTL-125 were tested for cytotoxicity onVero-E6 cells. 10 % DMSO v/v was used as a positive control for the induction of cytotoxicity and cell with no lectin was used as the negative control. The percent viability of cells was compared with the untreated cells. Final results from two biological repeats confirmed that ASAL treated cells were 100% viable at 10 μg/mL concentration whereas NTL-125 treated cells are above 95%viable at 5 μg/mL and 85% viable at 10 μg/mL concentration (Fig. S7).

The viral inhibitory properties of the lectins (ASAL and NTL-125) were assessed against SARS- CoV-2 multiplication in the Vero-E6 cell culture over the period of 48 hours. Inoculum of 1000 pfu was used to infect the Vero-E6 cells in presence or absence of lectins. Virus replication was inhibited fully even when NTL-125 concentration was gradually reduced from 20 μg/ml to 5 μg/ml yielding viral RNA in the supernatant to undetectable level (Fig. 2). The 50% inhibition of virus replication was observed at about 0.4 μg/mL NTL-125 (Fig. 2A). In comparison ASAL was found to be less potent than NTL-125 as 20 μg/mL of ASAL, showed only 80% reduction of viral replication with 50% inhibition occurring both at ~5 μg/mL and 10 μg/mL concentration (Fig. 2B. Niclosamide, a broad-spectrum antiviral agent (Xu et al., 2020), was used as a positive control in the viral inhibition assay. Niclosamide showed 100% inhibition at 1 μM concentration.

Inhibition of viral entry in ACE2-expressing cells

To assess whether the lectins, ASAL and NTL-125 act at the cell entry step of the virus or not, replication-incompetent HIV-1-based SARS-CoV-2 pseudo-virus (as described in the Methods section) was used in the assay. The study revealed that both NTL-125 and ASAL inhibited the entry of SARS-CoV-2 pseudo-virus in dose dependent manner. At 10 μg/mL concentration, NTL-125 and ASAL inhibited approximately to the extent of 90% and 70% respectively (Fig. 3 A). The inhibitory
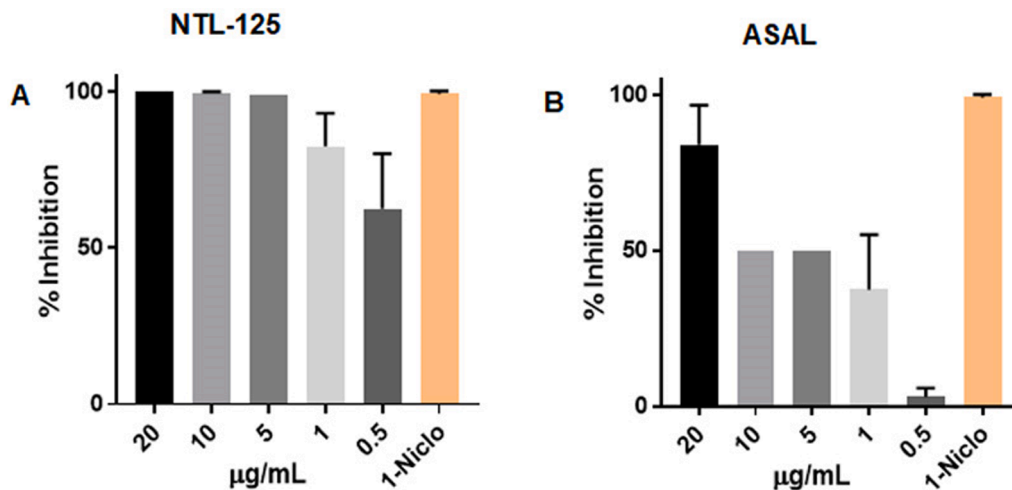
Fig. 2. Assessment of SARS CoV-2 inhibition in Vero-E6/TMPRSS2 cells by the lectins. Percentage of replication inhibition of SARS-CoV-2 by NTL-125 (A) and ASAL (B) lectins each at 0.5,1,5,10 and 20 μg concentrations indicated on X-axis. Each lectin assay was performed in two biological repeats with two technical repeats. The inhibition percentage calculation was based on increase in ct values. Niclosamide showed very high inhibition.
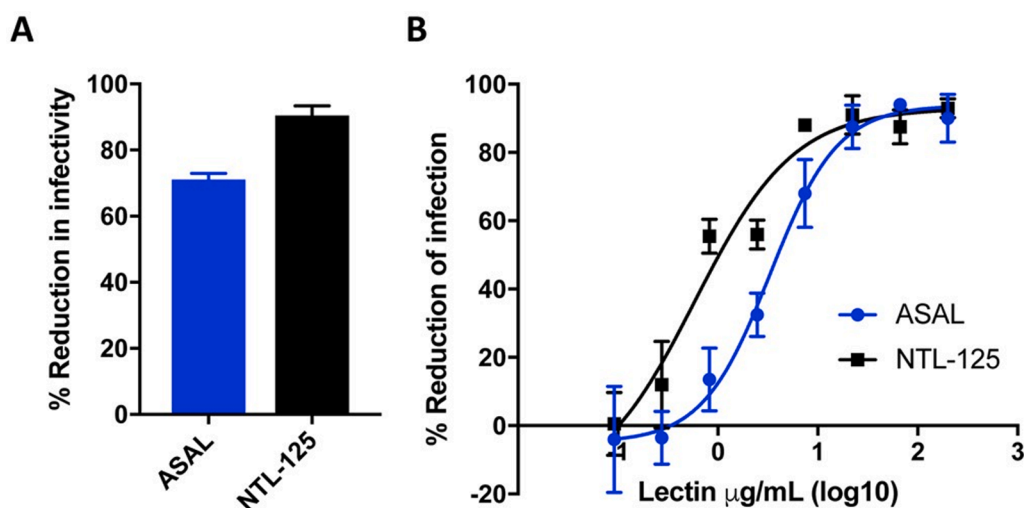

Fig. 3. Assessment of pseudotype virus inhibition in Vero-E6/TMPRSS2 cells by the lectins. ASAL and NTL-125 were tested in three biological repeats. Each assay was done using two technical repeats. (A) Percent reduction in infectivity by ASAL and NTL-125 at 10 μg/mL.Using the luminescence virus entry was measured at 2×10^5 RLU (Relative Luminescence Unit) of virus suspension. (B) Percent reduction in infectivity by ASAL and NTL-125 following serial dilution, measured by the luminescence at 2×10^5 RLU of virus suspension.

concentration that reduced the viral entry by 50% (IC_{50}) was approximately 4 and 0.8 μg/mL (i.e., 320 and 50 nM) for ASAL and NTL-125, respectively (Fig.3 B). The data are based on three independent repeat experiments.

In silico structural model building of the lectins

3D models of the lectins NTL-125 and ASAL were built based on the known X-ray structure of mannose binding lectin 3DZW as all three have high amino acid sequence similarities (Fig.1E). The stereo-chemical qualities of the built proteins were checked using Procheck (Laskowski et al., 1993) and Verify3D (Eisenberg et al., 1997). It showed that all residues of the three built proteins were within the allowed regions in the Ramachandran plots (Fig. S8). The verified 3D reports of NTL-125, ASAL and 3DZW-V36L showed compatibility score of 99.3%, 88.2% and 89.0% respectively, which indicate good qualities of the models (Fig. S8) suitable for docking studies. Superimpositions of the monomeric structures of NTL-125, ASAL and 3DZW-V36L reveal that, the structures of the proteins are more or less similar and comparable at monomeric orientation. However, NTL-125 has 30 residues C-terminal extension which triggers the formation of a helical structure (Fig. S9A). Both NTL-125 and 3DZW-V36L are homotetrameric proteins (Fig.4A,

4C) and ASAL a homodimeric one (Fig. 4B). Though NTL-125 and 3DZW-V36L monomers are quite similar, the presence of this C-terminal helix of NTL-125 makes it structurally dissimilar to both ASAL and 3DZW-V36L in the oligomeric form (Fig. 4A-C). The RMSD calculated between the backbone Cα-atoms of NTL-125 tetramer and 3DZW-V36L tetramer was therefore quite high (28.9 Å (Fig. S9A). The orientations of the N-terminal ends of the two proteins are however similar (Fig. S9 D, E).

In order to gain further support of the predicted NTL-125 structure, the homology model of NTL-125 was built using three independent web servers, Robetta (RED), SwissModel (GREEN) and Phyre2 (BLUE). Full chain NTL-125 model (residue 1 to 139) was built by Robetta only while models for the C-terminal truncated lectin (1-109) were built using SwissModel and Phyre2. These three structures were then superimposed and RMSD of the C-α backbone was calculated. The comparison shows very similar dispositions of secondary and tertiary structures (Fig. 4D) with RMSD ranging from 0.1 – 2.4 Å. It also supports that the predicted structure is software independent.

Docking of lectins with SARS-COV-2 spike protein

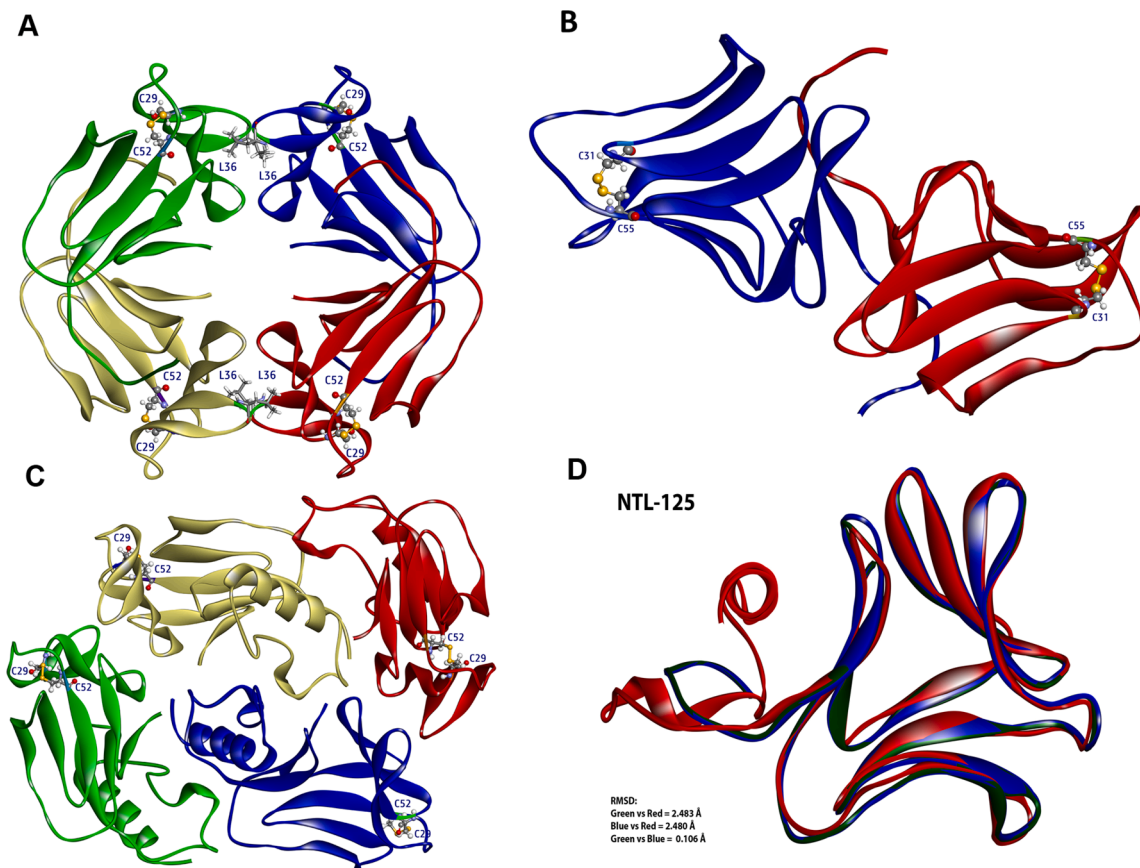The SARS-CoV-2 spike protein containing attached glycan moieties

Fig. 4. Multimeric structures of 3DZW-V36L, ASAL, NTL-125 and comparison of C-terminal and N-terminal domains of 3DZW-V36L, and NTL-125. (A) Homotetrameric structure of 3DZW-V36L, each chain is coded by different colours. (B) Homodimeric structure of ASAL, each chain is coded by different colours. (C) Homotetrameric structure of NTL-125, each chain is coded by different colours. (D) homology models of NTL-125 were built using three different servers, Robetta (RED), SwissModel (GREEN) and Phyre2 (BLUE). Full chain model (residue 1 to 139) was built by robetta, residues 1 to 109 were used for SwissModel and Phyre2. These three structures were superimposed and RMSD of the C-α backbone was calculated.

(Fig. S10 A, B) is a trimeric protein that contains an open receptor binding domain (RBD). The structure of the fully glycosylated spike protein was shown by Zhao et al. (2020) Residues 319–541 of the spike protein constitute the RBD and residues 438–508 constitute the Receptor Binding Motif (RBM). *In silico* docking simulation studies revealed that, among three lectins, only NTL-125 is able to bind to the RBM efficiently (Fig. 5A-D) similar to that of the hACE-2 protein (Fig. 5E-H).

The docked structure also revealed that thirty-six residues of RBD and 44 residues of NTL-125 (Table 1) were located within 5Å distance from each other in the complex whereas 27 residues of ACE-2 are in proximity to 32 residues of RBD. There are 17 common residues of RBD (marked bold in Table 1) that interact with both ACE-2 and NTL-125. Among all these residues, 10 of RBD and 11 of NTL-125 are within 3Å distance in the docked structure. For the RBD: ACE-2 complex, 9 residues of RBD and 9 residues of ACE-2 are within 3Å distance. NTL-125 occupies exactly the same region of the receptor binding motif (RBM) of the spike protein where hACE2 usually binds (Fig. 6A). The docked complex between NTL-125 and Spike revealed that among the four chains of NTL-125, only three (Chain T, V and W) actively participate in the interactions with the spike protein within 3Å (Fig. 6 B-D and Table 1). The binding free energy change of NTL125–S-protein interaction (-13.3 kcal/mol, k_d 0.41nM, Table 2) is more negative than that between S-protein-hACE2 (-11.2 kcal/mol, $k_d \sim 12$ nM) which clearly indicates that the former is more stable than the later. ASAL-Spike complex showed the lowest binding free energy change (16kcal/mol, $k_d \sim 0.005$nM) but the zone of this interaction is outside the RBD (Fig. S11 A-D). As a result, the RBD remained open for any possible interaction with hACE2. For the 3DZW-Spike complex $\Delta G = -12.2$ kcal/mol and

$k_d = 2.5$ nM, but the interaction is again outside the RBD (Fig. S12 A-D).

Docking study confirmed that the interaction between NTL-125-spike protein is also mediated through a S-protein glycan moiety, covalently linked to Asn125 of the spike protein and interacts with Ile137 and Thr138 of NTL-125 protein (Fig. 6E). Thus, the interaction between NTL-125-Spike is not only through amino acid residues but also through the glycan moieties. This finding is significant because glycan interaction mechanism is believed to play a crucial role in the viral evolution and cell entry of the virus (Shang et al., 2020). Glycan shield of viral surface protects the virus (Hao et al., 2021; Kosik et al., 2018) but NTL-125 antagonizes the shielding effect using these glycans as a target making it an effective antiviral agent.

Docking analysis of mutated NTL-125 with Spike RBD protein

The structures of different mutants of NTL-125 were generated and individually docked with the spike RBD. We were especially interested to study the effect of the C-terminal (110-139) truncation of NTL-125 (NTL-C-delta) on its binding with the RBD of the spike protein. In Figure 7 A and B we compared the zone of interaction of NTL-125 and NTL-C-delta mutant with the RBD. The residues of RBD within the zone of interaction with NTL are summarized in Table S2. We mentioned earlier that 36 residues of RBD including 32 residues of RBM are within the zone of interaction with full length NTL-125. But when the NTL-125 is stripped off residues 110-139 from the C-terminal, only 23 residues of RBD (all within RBM) are within the zone of interaction. The 13 residues of RBD including 9 residues from RBM that moves out of the zone of interactions with NTL-C-delta are: A348, S349, T351, A352, G450,
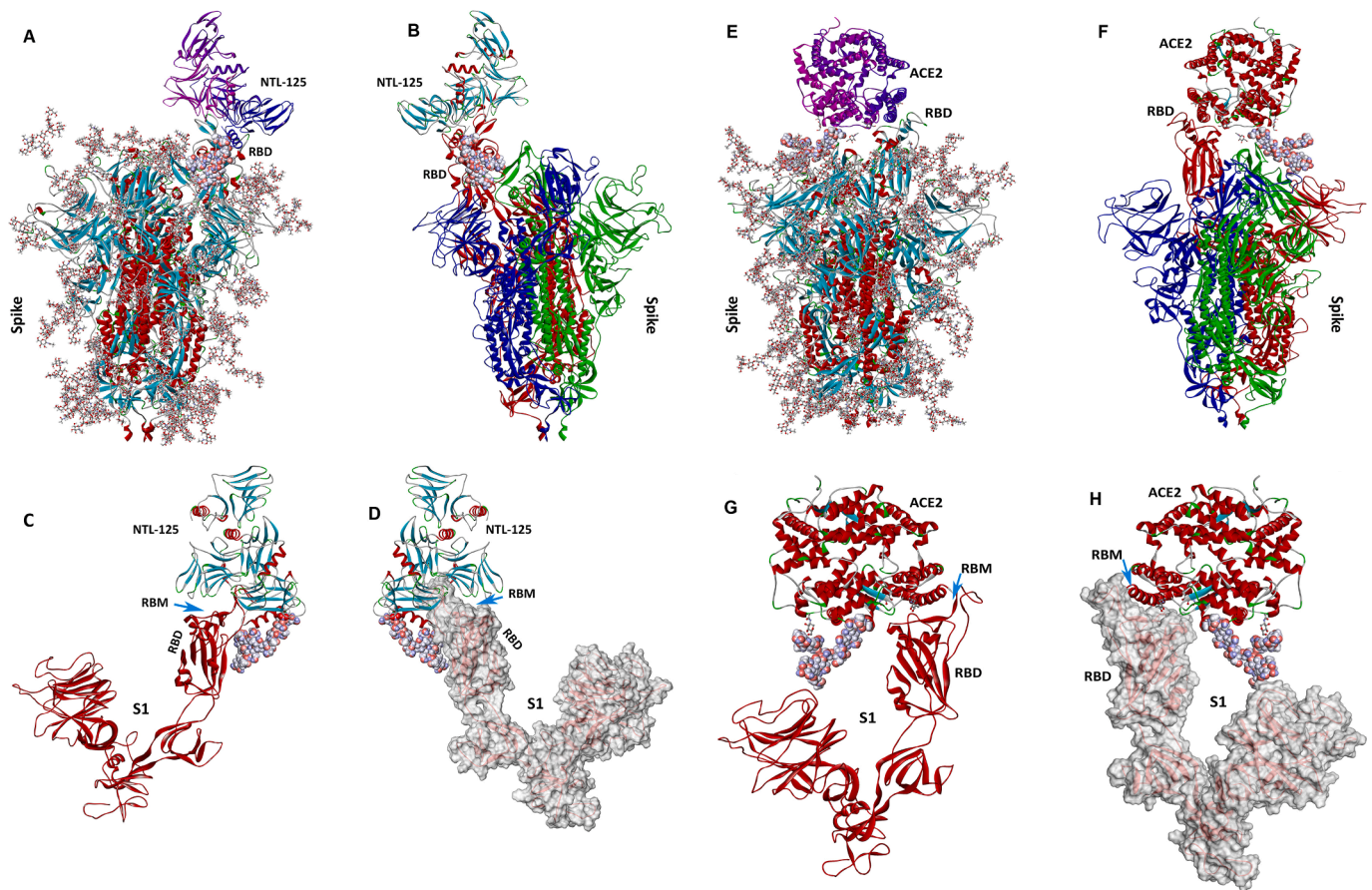
Fig. 5. Docked representations of SARS-CoV-2 Spike-NTL-125 complexes and SARS-CoV-2 Spike-hACE2 complexes. The proteins are in ribbon model; the glycans are in stick model; and the glycan molecule interacting with both NTL-125 and spike is in CPK model. (A) NTL-125 bound with Spike protein. (B) NTL-125 bound with the Spike protein (Red colour open RBD chain). ((C, D) Zoomed view of NTL-125 and S1 region of the spike protein in 180°rotational view. (E) ACE2 bound with Spike protein. (F) ACE2 bound with the Spike protein (Red colour open RBD chain). (G, H) Zoomed view of ACE2 and S1 region of the spike protein in 180° rotational view.

Table 1

Interacting residues of Spike protein in 5Å radius, bound with NTL-125 and ACE2 (Underlined ones are in 3Å radius). Residues marked in bold are common interacting residues.

Ligand	Interacting residues of S-protein at RBD	Receptor	Interacting residues of the receptor
Wild Type Spike Protein	A348, S349, Y351, A352, V445, G446, G447, Y449, N450, Y451, L452, T470, Q471, I472, S477, T478, P479, C480, N481, G482, V483, E484, G485, F486, N487, C488, Y489, F490, P491, L492, Q493, Q498, P499, T500, N501, G502	NTL-125	Chain V : R20, L36, K90, R92, P117, G118, S119, A120, P121, Q122, N123, E127, L131, K139, Chain T : P12, G13, E27, R50, R51, H109, Chain W : Y5, S6, G7, Q57, S58, E80, N81, G82, N83, Y84, T99, A100, R101, W102, A103, G105, T106, N107, I108, H109, G110, A111, G112, I113
	R403, K417, V445, G446, G447, Y449, Y453, L455, F456, Y473, A475, G476, S477, E484, F486, N487, Y489, F490, L492, Q493, S494, Y495, G496, F497, Q498, P499, T500, N501, G502, V503, G504, Y505	hACE2	S19, E23, Q24, T27, F28, D30, K31, H34, E35, E37, D38, Y41, Q42, L45, L79, M82, Y83, T324, Q325, G326, N330, L351, K353, G354, D355, R357, R393

T451, L452, T470, Q471, I472, G482, P491 and L492. Loss of C-terminal of NTL-125, in particular I137 and T138 also eliminates the interaction of glycan moiety attached to Asn125 of spike protein. Loss of these crucial interactions leads to substantial reduction in binding affinity and binding free energy. The binding affinity and energy values of all the mutant NTL-125 with RBD were presented in Table 3. The binding interaction of wild type NTL-125 with RBD was found to be stronger than all the mutants including that of C-terminal truncated mutant. The C-terminal truncated mutant showed a binding energy loss of 2.3 kcal/mol indicating that the C-delta mutant of NTL-125 did not bind to RBD as strongly as the wild type NTL-125 justifying the importance of the C-terminal tail in the binding interaction. Apart from the C-terminal region, the single point alanine mutations in the region between 81-83 residues expectedly produced small but significant energy differences in the range of 0.2-0.5 kcal/mol while alanine mutation at residue 80 produced negligible energy changes (0.1 kcal/mol). This mutation data supports the identification of the residues 80-84 and the 15 other residues located in the C-terminal tail region (Table 1) important for interaction with the RBD of the spike protein.

Discussion

Plant lectins are a group of storage proteins accumulated in organs like bulbs, leaves, rhizomes etc. and are ubiquitously present in almost all life forms. They serve as defense proteins when needed and protect the host plants from insect and pathogen attack. Mannose binding plant lectins isolated from Amaryllidaceae and Alliaceace family exhibited
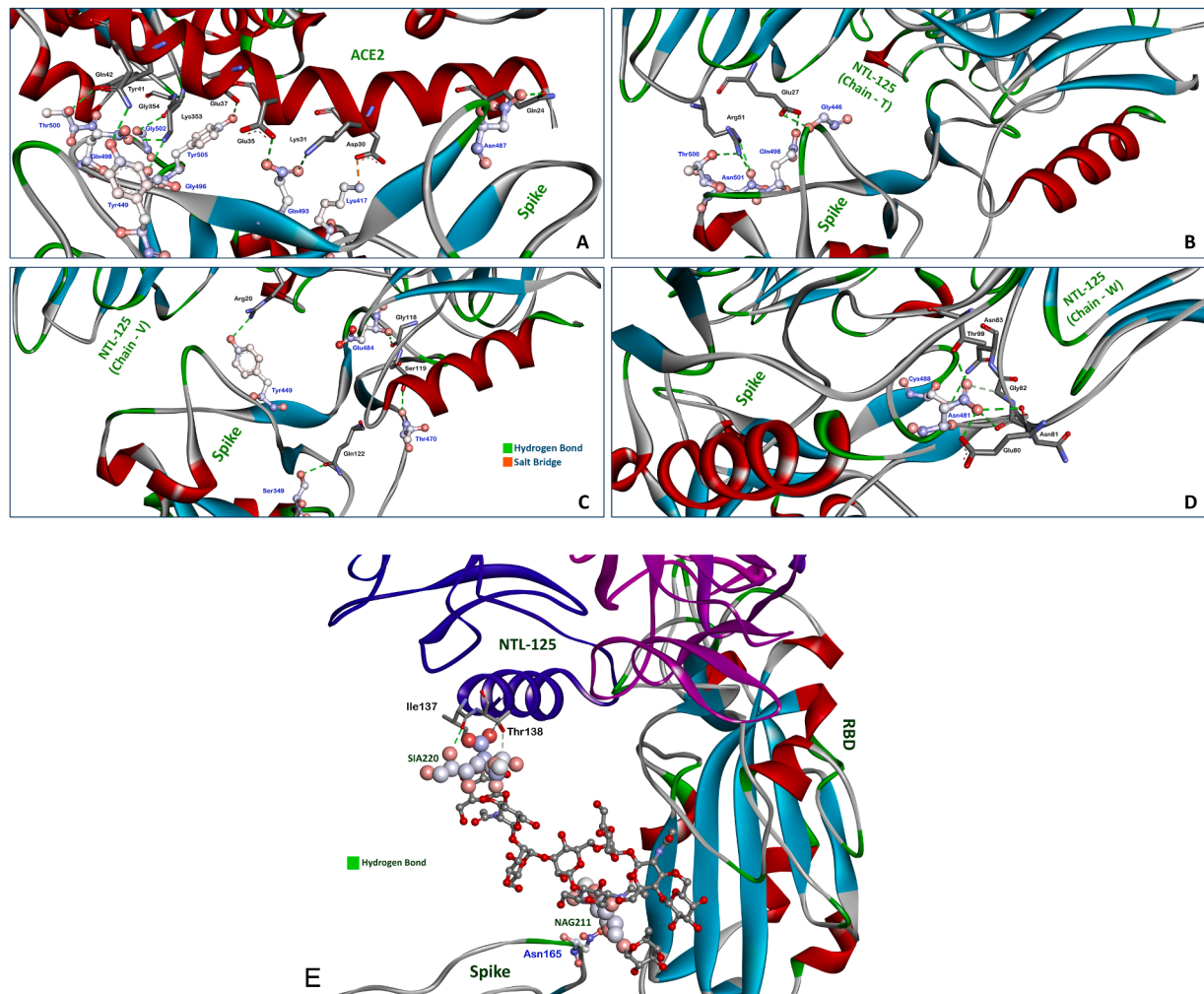
Fig. 6. Zoomed views of the binding clefts of the spike-ACE2 and spike-NTL-125 complexes. The residues of spike are displayed as ball and stick model, and the residues of ACE2 and NTL-125 are displayed as stick model. (A) ACE2 interacting with spike protein. (B) T chain of the tetrameric NTL-125 is interacting with spike. (C) V chain of the tetrameric NTL-125 is interacting with spike. (D) W chain of the tetrameric NTL-125 is interacting with spike. (E). Involvement of glycan in SARS-CoV-2 spike-NTL-125 complex formation. The proteins are in ribbon model, the glycan is in ball and stick model.

Table 2
Binding free energy of different Spike mutants, bound with ACE2 and NTL-125.

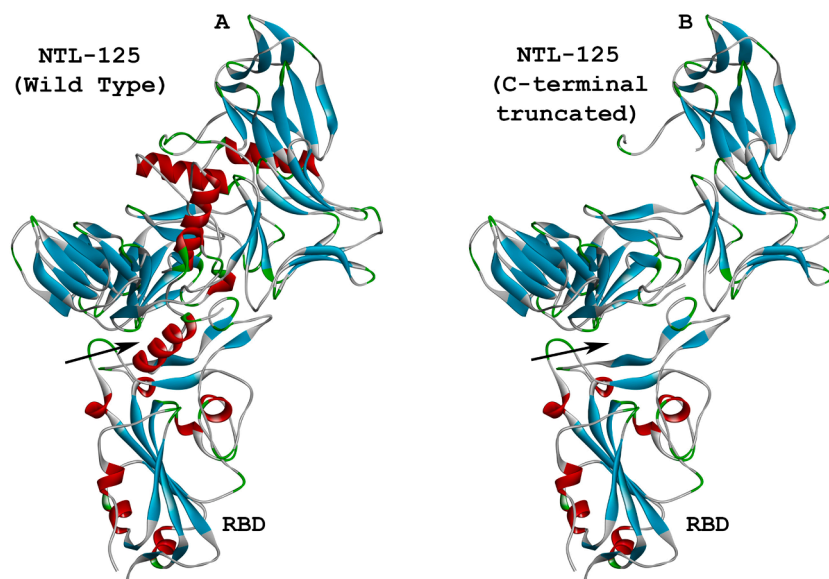| Sl. No.	Mutations	ACE2-Spike Mutant (ΔG in kcal/mol)	Kd (nM) at 37.0 °C	RMSD of ACE2-Spike complex (Å)	NTL125-Spike Mutant (ΔG in kcal/mol)	Kd (nM) at 37.0 °C	RMSD of NTL125-Spike complex (Å)	Gain of free energy (ΔΔG)
Wild type Spike	-	-11.20	12.0		-13.30	0.41		-2.10
Mutant 1	K417N, D614G	-11.88	4.21	0.21	-13.09	0.59	0.16	-1.21
Mutant 2	K417T, D614G	-11.90	4.12	0.11	-12.44	1.70	0.40	-0.54
Mutant 3	L452R, D614G	-11.94	3.84	0.12	-12.97	0.72	0.18	-1.03
Mutant 4	N440K, D614G	-11.91	4.03	0.23	-13.25	0.46	0.18	-1.33
Mutant 5	E484K, D614G	-11.74	5.31	0.22	-12.94	0.75	0.20	-1.21
Mutant 6	E484Q, D614G	-11.51	7.74	0.18	-12.94	0.76	0.17	-1.43
Mutant 7	N501Y, D614G	-11.59	6.72	0.24	-13.62	0.25	0.19	-2.03
Mutant 8	D614G	-12.11	2.91	0.28	-12.98	0.71	0.17	-0.87
Mutant 9	D614G, P681H	-11.87	4.32	0.12	-12.71	1.10	0.38	-0.84
Mutant 10	D614G, P681R	-11.62	6.43	0.19	-12.95	0.74	0.18	-1.33
Mutant 11	G142D, E154K, L452R, E484Q, D614G, P681R, Q1071H	-11.53	7.40	0.20	-12.71	1.10	0.25	-1.17
Mutant 12	S477G, D614G	-11.75	5.21	0.13	-13.35	0.39	0.17	-1.60
Mutant 13	S477N, D614G	-11.75	5.21	0.23	-13.27	0.44	0.18	-1.52

Fig. 7. Docking representations of wild type and C-terminal del mutant of NTL-125 with spike protein. (A) Full length NTL-125 bound with Spike protein (B) C-terminal del mutant bound with Spike protein.

Table 3
Binding free energy (∆G) profile of different mutant of NTL-125 with Spike protein.

Sl. No.	Mutation in NTL-125	NTL125-Spike (ΔG^o in kcal/mol)	K_d (nM) at 37°°C	$\Delta\Delta G^o$ (Kcal/ mol)
Wild type	___	-13.32	0.41	___
Mutant 1	GLU80ALA	-13.26	0.448	
				+ 0.06
Mutant 2	ASN81ALA	-13.09	0.590	
				+ 0.23
Mutant 3	GLY82ALA	-13.14	0.544	
				+ 0.18
Mutant 4	ASN83ALA	-12.80	0.945	
				+ 0.52
Mutant 5 C-Terminal delta -Mutant	Delta 110-139	-10.99	17.84	
				+ 2.33

antiviral property against human disease-causing viruses (Balzarini, 2005). Similarly, *Narcissus tazetta* lectin (NTL) showed strong inhibitory effect against human respiratory syncytial virus, influenza A (H1N1, H3N2, H5N1) and influenza B viruses (Ooi *et al* 2010). Lately monocot mannose-binding lectins, which belong to a superfamily of structurally and evolutionarily related proteins have earned growing attention due to their antiviral activities against several other human disease-causing viruses namely, immunodeficiency virus (HIV), human cytomegalovirus (HCMV), hepatitis C virus (HCV), herpes simplex virus type 1 (HSV-I), herpes simplex virus type 2 (HSV-2), virus, and coronavirus (SARS-CoV) etc.

In the present investigation a newly identified tetrameric NTL-125 protein (accession number COHU1) the sequence of which differs from the earlier reported protein NTL (PDB id: 3DZW) and contains an additional C-terminal helical stretch and a change in amino acid at 36th position i.e., V36L is studied for antiviral activity. The sequence was confirmed through differential LC-MS analyses. Accordingly, the structure of the protein was built based on the homology modelling on the reported crystal structure (PDB id: 3DZW). As a significant characteristic, NTL-125 agglutinated rabbit erythrocyte efficiently at an optimum

temperature of 30-37°C. More interestingly, NTL-125 demonstrated inhibitory effect on SARS-CoV-2 viral replication in Vero-E6 cell line. The Ct value of virus replication in Vero cells reduced significantly when artificially inoculated with live virus pre-incubated with NTL-125 as compared to untreated virus or virus pre-treated with ASAL. Previous study showed antiviral activity of lectin against human HINI, H3N2 with EC$_{50}$ values ranging between 0.02μg/mL and 1.33 μg/mL (Ooi et al., 2010). Compared to that, present NTL-125 showed IC$_{50}$ value of ~0.6 μg/mL against SARS-CoV-2.

Previously Keyaerts et al., (2007) also showed that different plant lectins showed antiviral activities against SARS-COV with IC$_{50}$ ranging from 1 to 100 μg/mL. Interestingly, the IC$_{50}$ value for viral entry inhibition obtained for NTL-125 (i.e., 50nM) is similar to that of SARS-CoV-2 RBD specific monoclonal antibodies (Chen et al., 2020) that effectively neutralized pseudo-virus entry with IC$_{50}$ ranging between 34-70 nM. These results re-establish the therapeutic potential of lectins and confirm that NTL-125 is the more potent one between the two lectins studied here.

The interaction with the receptor binding domain of spike protein is the determining factor for SARS CoV-2 virus infection (Shang et al., 2020). *In vitro* analyses of the virus replication assay in human cell exhibited significant reduction of the viral replication by NTL-125 at a very low concentration. Docking experiments conducted on spike protein with three lectins (ASAL, NTL-125 and 3DZW-V36L) revealed that all the lectins interact with spike protein (Fig. 5, S11, S12) but only NTL-125 showed stable binding with RBD. Significantly lower free energy between NTL-125 and RBD interaction was observed compared to the same between RBD and ACE-2 due to higher number of interacting residues (36 of RBD and 44 of NTL-125 in contrast to 32 of RBD and 27 of hACE-2) within 5Å distance zone, respectively. Also, more negative binding free energy during interaction between NTL125-spike protein than that between spike protein-hACE2 suggests more stable binding in the case of former interaction. The sub-nanomolar binding constant indicates strong binding of NTL-125 with the S-protein. It may be mentioned here that many human monoclonal antibodies that effectively neutralized SARS-CoV-2 have binding constants in the nanomolar range (Wang et al., 2020).

NTL-125 has more antiviral potential than ASAL. Multiple Sequence Alignment (MSA) of NTL-125, ASAL and 3DZW-V36L (Fig. S13A) was performed to analyze the relative positions of the corresponding interacting amino acid residues. The highlighted residues (in black

background) of NTL-125 interact with the spike protein. It again shows that the C-terminal extended region of NTL-125 protein is primarily responsible for the interaction with the spike protein as out of the 30 residues (residues 110-139) of the terminal extension 14 residues (chain W: 110-113; chain V: 117-123, 127,131, 139) are found within the 5Å interaction zone of RBD (Table 2). It has been experimentally demonstrated in the literature that helical peptides are strong inhibitors of interaction between the spike protein and hACE2 (Shang et al., 2020). This makes NTL-125 uniquely suitable as antiviral protein against SARS-CoV-2.

Further support for the importance of the C-terminal region of NTL-125 in its interaction with RBD was obtained from the docking study of RBD with *in silico* mutated NTL-125 (Table 3). Elimination of the C-terminal tail (110-139) significantly reduced the binding affinity as observed by more than 40-fold increase in the dissociation constant (Table 3). The stretch 81-83 identified within the RBD interaction zone was also verified by the *in-silico* mutation study as replacing the respective single residues by alanine led to loss of binding affinity in all cases. Thus, the *in-silico* NTL-125 mutation data is consistent with identification of the interacting residues given in Table 1.

Soon after being discovered in Wuhan, SARS-CoV-2 mutated with changes D614G, and E484K, showing increased infectivity, immunosuppression, and reinfection properties. Gradually various strains such as B.1.1.7 with deletion of residues 69-70 with P681H mutation, B.1.351 (501.V2) with N501Y mutation, B.1.617 with G142D, E154K, L452R, E484Q, D614G, P681R, Q1071 H mutations, B.1.618 with E484K mutation and many other, were identified in various countries. Mutations led to some changes in the key amino acids of the spike protein resulting in altered binding efficiency with hACE2 receptor as shown in Table S1. Fast evolving SARS-CoV-2 variants having increased binding efficiency to hACE2 are imposing threat to human beings with capabilities of immune escape, super virulence and higher infectivity features (Korber et al., 2020; Tegally et al., 2021) leading to increased fatality rate (Table S1). Recently Shang et al., (2020) demonstrated that increased transmissibility is correlated with the higher binding affinity of the mutants to hACE2. Rapid rate of viral mutations and immune escape capability currently are of great concern as to whether the vaccines would remain effective over a long period under this quickly changing scenario. Currently many countries are facing these challenges where death toll has gone up significantly.

Individual docking approach has been undertaken for several mutated spike proteins interacting with NTL-125 and hACE2 separately which showed no significant RMSD changes for the complexes (Table 2.) Interestingly, all the mutant spike with NTL-125 complexes showed lower free energy changes and higher binding affinity compared to the corresponding mutant spike -hACE-2 complexes. The gain in free energy ($\Delta\Delta G$) of the mutant spike -NTL-125 complexes over that of the mutant spike -hACE2 complexes in most of the studied cases are quite significant and over 1 kcal/mole (Table 2) except for spike mutant number 2, 8 and 9. Mutant 7 (N501Y, D614G) showed the maximum $\Delta\Delta G$ of 2.0 kcal/mol and the binding involves 3 more amino acids (V: D35, T: S11 and T: H53) compared to the original (wild type) spike protein interaction. This particular mutant variant is responsible for increased infectivity (Table S1), through altered binding pattern with hACE2. Our data shows that NTL-125 can be most effective against this particular mutant. Mutant 5 (E484K, D614G), also responsible for increased infectivity, showed effective binding with NTL-125 with all native residues along with 2 more amino acids from NTL-125 (T104 and K139). Interacting residues of mutant spike proteins within 3Å and 5Å radius, bound with NTL-125 and bound with ACE2 were also identified. For Mutant 5 and 11, one extra amino acid K444 on spike protein was found to interact with NTL-125. For Mutant 12 and 13, Q474 of spike protein was found to interact with NTL-125 but two residues, A352, K444 that were absent in wild type spike protein containing strain do not have any interaction with NTL-125. Mutants 1, 2, 3, 4 and 5 showed impaired interaction at L492 and S494 positions with hACE2 (Table 1). Likewise, Mutants 7, 9, 10, 11

and 13 showed impaired interactions for the respective (P499, G504), (S494, G504), S494, L492 and S494 amino acid residues. Docking study also demonstrated that mutants 4, 5, 7, 8 and 13 attained additional interaction ability mediated by Y421 residue. Table 2 shows the comparative analyses of various ACE2-Spike and NTL-125-Spike complexes in terms of differences of binding free energy and K_d values. The data clearly show that NTL-125-mutant spike protein interaction is thermodynamically more favorable than the corresponding ACE2-mutant interaction. This ensures that NTL-125 can efficiently inhibit all the mutants including Delta Plus spike variant / Mutant 1 (K417N) from attaching itself to hACE2 protein.

Conclusion and future perspective

Overall, our data demonstrate that mannose binding monocot plant lectin, NTL-125 interacts with SARS-CoV-2 and all its mutant variants with higher efficiency compared to hACE2 so that the virus would be captured by the NTL-125 blocking the path to its entry into the host. We have shown that NTL-125 is uniquely suitable for the antiviral activity against SARS-CoV-2 among three lectins studied here because of (i) the existence of unique 30 residue C-terminal helical tail region that strongly interacts with RBD; (ii) the zone of interaction of RBD with NTL-125 significantly overlaps with that of hACE2. Since the RBD-NTL-125 interaction is of higher affinity than the RBD-hACE2 interaction, NTL-125 can prevent the virus from binding to the ACE2 receptor and thus block cell entry; (iii) NTL-125 can also recognize and more effectively bind even the mutated spike proteins that is continuously evolving;(iv) its special ability to interact with some glycan moieties of S-protein disrupting the protective viral shield and strengthening the binding interaction. Both experimental and *in silico* data firmly establish the therapeutic potential of NTL-125 towards the possible management of COVID-19. Being a glycoprotein bio-macromolecule from plant origin, NTL-125 can be an environmentally safe candidate as found from the cytotoxicity data. There is immense biotechnological potential to develop NTL-125 based anti-COVID-19 agent as well as a COVID-19 detection kit in this continuously changing pandemic scenario. Through this investigation, we would like to establish the efficacy of the novel lectin NTL-125 against SARS-CoV-2. The possible mode of administration of this novel lectin NTL-125 either intramuscularly or intranasally is subjected to further research.

Funding

CRediT authorship contribution statement

SD and AS conceived the idea and wrote the manuscript. SP, PN and SwD purified the protein. SP and PN carried out mass spectrometric analyses. CS, SK, DKD, AS, KGT and RPR performed the virus study. SD, AS and DD designed the experiments. AB and NC did the structural modeling and performed the Docking experiment. AB and RPR took part in initial manuscript drafting. SS took part in analyzing the data. KpD analyzed the data and was involved in final drafting of the manuscript.

Declaration of interests

The authors declare that they have no known competing financial interests or personal relationships that could have appeared to influence the work reported in this paper.

Declaration of competing interests

Authors declare that they do not have any financially or academically competing interest involved in this study.

Supplementary materials

Supplementary material associated with this article can be found, in the online version, at doi:10.1016/j.virusres.2022.198768.

References

Abraham, M.J., Murtola, T., Schulz, R., Páll, S., Smith, J.C., Hess, B., Lindahl, E., 2015. GROMACS: High performance molecular simulations through multi-level parallelism from laptops to supercomputers. SoftwareX 1–2, 19–25. https://doi.org/10.1016/j.softx.2015.06.001.

Balzarini, J., 2006. Inhibition of HIV entry by carbohydrate-binding proteins. Antiv. Res. 71, 237–247. https://doi.org/10.1016/j.antiviral.2006.02.004.

Balzarini, J., Neyts, J., Schols, D., Hosoya, M., Van Damme, E., Peumans, W., De Clercq, E., 1992. The mannose-specific plant lectins from Cymbidium hybrid and Epipactishellebrone and the (N-acetylglucosamine) n-specific plant lectin from Urticadioica are potent and selective inhibitors of human immunodeficiency virus and cytomegalovirus replication in vitro. Antiv. Res. 18, 191–207 https://doi.org/10.1016/0166-3542(92)90038-7.

Balzarini, J., Van Laethem, K., Hatse, S., Froeyen, M., Peumans, W., Van Damme, E., Schols, D., 2005. Carbohydrate-binding Agents Cause Deletions of Highly Conserved Glycosylation Sites in HIV GP120. J. Biol. Chem. 280, 41005–41014 https://doi.org/10.1074/jbc.M508801200.

Bandyopadhyay, S., Roy, A., Das, S., 2001. Binding of garlic (Allium sativum) leaf lectin to the gut receptors of homopteran pests is correlated to its insecticidal activity. Plant Sci. 161, 1025–1033 https://doi.org/10.1016/S0168-9452(01)00507-6.

Banerjee, S., Hess, D., Majumder, P., Roy, D., Das, S., 2004. The interactions of allium sativum leaf agglutinin with a chaperonin group of unique receptor protein isolated from a bacterial endosymbiont of the mustard aphid. J. Biol. Chem. 279, 23782–23789 https://doi.org/10.1074/jbc.M401405200.

Benson, D.A., Cavanaugh, M., Clark, K., Karsch-Mizrachi, I., Lipman, D.J., Ostell, J., Sayers, E.W., 2012. GenBank. Nucl. Acids Res. 41, D36–D42 https://doi.org/10.1093/nar/gks1195.

Berendsen, H.J.C., Grigera, J.R., Straatsma, T.P., 1987. The missing term in effective pair potentials. J. Phys. Chem 91, 6269–6271 https://doi.org/10.1021/j100308a038.

Brooks, B.R., Bruccoleri, R.E., Olafson, B.D., States, D.J., Swaminathan, S., Karplus, M., 1983. CHARMM: a program for macromolecular energy, minimization, and dynamics calculations. J. Comput. Chem. 4, 187–217 https://doi.org/10.1002/jcc.540040211.

Cai, Y., Zhang, J., Xiao, T., Peng, H., Sterling, S.M., Walsh, R.M., Rawson, S., Rits-Volloch, S., Chen, B., 2020. Distinct conformational states of SARS-CoV-2 spike protein. Science 369, 1586–1592 https://doi.org/10.1126/science.abd4251.

Caly, L., Druce, J.D., Catton, M.G., Jans, D.A., Wagstaff, K.M., 2020. The FDA-approved drug ivermectin inhibits the replication of SARS-CoV-2 in vitro. Antiv. Res. 178, 104787 https://doi.org/10.1016/j.antiviral.2020.104787.

Chakraborti, D., Sarkar, A., Mondal, H.A., Das, S., 2009. Tissue specific expression of potent insecticidal, Allium sativum leaf agglutinin (ASAL) in important pulse crop, chickpea (Cicerarietinum L.) to resist the phloem feeding Aphis craccivora. Transgenic Res. 18, 529–544 https://doi.org/10.1007/s11248-009-9242-7.

Chen, X., Li, R., Pan, Z., Qian, C., Yang, Y., You, R., Zhao, J., Liu, P., Gao, L., Li, Z., Huang, Q., Xu, L., Tang, J., Tian, Q., Yao, W., Hu, L., Yan, X., Zhou, X., Wu, Y., Deng, K., Zhang, Z., Qian, Z., Chen, Y., Ye, L., 2020. Human monoclonal antibodies block the binding of SARS-CoV-2 spike protein to angiotensin converting enzyme 2 receptor. Cell MolImmunol 17, 647–649 https://doi.org/10.1038/s41423-020-0426-7.

Coughlin, M.M., Babcook, J., Prabhakar, B.S., 2009. Human monoclonal antibodies to SARS-coronavirus inhibit infection by different mechanisms. Virology 394, 39–46 https://doi.org/10.1016/j.virol.2009.07.028.

Das, A., Roy, A., Mandal, A., Mondal, H.A., Hess, D., Kundu, P., Das, S., 2021. Inhibition of Bemisiatabaci vectored, GroEL mediated transmission of tomato leaf curl New Delhi virus by garlic leaf lectin (Allium sativum leaf agglutinin). Virus Res. 300, 198443 https://doi.org/10.1016/j.virusres.2021.198443.

David, A.B., Diamant, E., Dor, E., Barnea, A., Natan, N., Levin, L., Chapman, S., Mimran, L.C., Epstein, E., Zichel, R., Torgeman, A., 2021. Identification of SARS-CoV-2 receptor binding inhibitors by in vitro screening of drug libraries. Molecules 26, 3213 https://doi.org/10.3390/molecules26113213.

Dutta, I., Majumder, P., Saha, P., Ray, K., Das, S., 2005a. Constitutive and phloem specific expression of Allium sativum leaf agglutinin (ASAL) to engineer aphid (Lipaphiserysimi) resistance in transgenic Indian mustard (Brassica juncea). Plant Sci. 169, 996–1007 https://doi.org/10.1016/j.plantsci.2005.05.016.

Dutta, I., Saha, P., Majumder, P., Sarkar, A., Chakraborti, D., Banerjee, S., Das, S., 2005b. The efficacy of a novel insecticidal protein, Allium sativum leaf lectin (ASAL), against homopteran insects monitored in transgenic tobacco. Plant Biotechnol. J. 3, 601–611 https://doi.org/10.1111/j.1467-7652.2005.00151.x.

Eisenberg, D., Lüthy, R., Bowie, J.U., 1997. [20]VERIFY3D: Assessment of protein models with three-dimensional profiles. Methods in Enzymology. Elsevier, pp. 396–404 https://doi.org/10.1016/S0076-6879(97)77022-8.

Gao, Q., Bao, L., Mao, H., Wang, L., Xu, K., Yang, M., Li, Yajing, Zhu, Ling, Wang, N., Lv, Z., Gao, H., Ge, X., Kan, B., Hu, Y., Liu, J., Cai, F., Jiang, D., Yin, Y., Qin, Chengfeng, Li, J., Gong, X., Lou, X., Shi, W., Wu, D., Zhang, H., Zhu, Lang, Deng, W., Li, Yurong, Lu, J., Li, C., Wang, X., Yin, W., Zhang, Y., Qin, Chuan, 2020. Development of an inactivated vaccine candidate for SARS-CoV-2. Science 369, 77–81 https://doi.org/10.1126/science.abc1932.

Gatehouse, A., Powell, K., Van Damme, E., Gatehouse, J., 1995. Insecticidal properties of plant lectins. In: Pusztai, A., Bardocz, S. (Eds.), Lectins - Biomedical Perspectives. Taylor & Francis, London, UK, pp. 29–48.

Gundry, R.L., White, M.Y., Murray, C.I., Kane, L.A., Fu, Q., Stanley, B.A., Van Eyk, J.E., 2009. Preparation of proteins and peptides for mass spectrometry analysis in a bottom-up proteomics workflow. In: Ausubel, F.M., Brent, R., Kingston, R.E., Moore, D.D., Seidman, J.G., Smith, J.A., Struhl, K. (Eds.), Current Protocols in Molecular Biology. John Wiley & Sons, Inc., Hoboken, NJ, USA https://doi.org/10.1002/0471142727.mb1025s88.

Gurevich, E.V., Gurevich, V.V., 2014. Therapeutic potential of small molecules and engineered proteins. HandbExpPharmacol 219, 1–12 https://doi.org/10.1007/978-3-642-41199-1_1.

Hao, W., Ma, B., Li, Z., Wang, X., Gao, X., Li, Y., Qin, B., Shang, S., Cui, S., Tan, Z., 2021. Binding of the SARS-CoV-2 spike protein to glycans. Sci. Bull. 66, 1205–1214 https://doi.org/10.1016/j.scib.2021.01.010.

Ho, T., Wu, S., Chen, J., Li, C., Hsiang, C., 2007. Emodin blocks the SARS coronavirus spike protein and angiotensin-converting enzyme 2 interaction. Antiv. Res. 74, 92–101 https://doi.org/10.1016/j.antiviral.2006.04.014.

Ho, T., Wu, S., Chen, J., Wei, Y., Cheng, S., Chang, Y., Liu, H., Hsiang, C., 2006. Design and biological activities of novel inhibitory peptides for SARS-CoV spike protein and angiotensin-converting enzyme 2 interaction. Antiv. Res. 69, 70–76 https://doi.org/10.1016/j.antiviral.2005.10.005.

Huang, Y., Yang, C., Xu, X., Xu, W., Liu, S., 2020. Structural and functional properties of SARS-CoV-2 spike protein: potential antivirus drug development for COVID-19. ActaPharmacol Sin 41, 1141–1149 https://doi.org/10.1038/s41401-020-0485-4.

Kachko, A., Loesgen, S., Shahzad-ul-Hussan, S., Tan, W., Zubkova, I., Takeda, K., Wells, F., Rubin, S., Bewley, C.A., Major, M.E., 2013. Inhibition of Hepatitis C Virus by the Cyanobacterial Protein *Microcystisviridis* Lectin: Mechanistic Differences between the High-Mannose Specific Lectins MVL, CV-N, and GNA. Mol. Pharmaceutics 10, 4590–4602 https://doi.org/10.1021/mp400399b.

Kadam, R.U., Wilson, I.A., 2017. Structural basis of influenza virus fusion inhibition by the antiviral drug Arbidol. Proc. Natl. Acad. Sci. USA 114, 206–214 https://doi.org/10.1073/pnas.1617020114.

Kaku, H., Van Damme, E.J., Peumans, W.J., Goldstein, I.J., 1990. Carbohydrate-binding specificity of the daffodil (Narcissus pseudonarcissus) and amaryllis (Hippeastrum hybr.) bulb lectins. Arch BiochemBiophys 279, 298–304 https://doi.org/10.1016/0003-9861(90)90495-k.

Keeffe, J.R., Gnanapragasam, P.N.P., Gillespie, S.K., Yong, J., Bjorkman, P.J., Mayo, S.L., 2011. Designed oligomers of cyanovirin-N show enhanced HIV neutralization. Proc. Natl. Acad. Sci. 108, 14079–14084 https://doi.org/10.1073/pnas.1108777108.

Keyaerts, E., Vijgen, L., Pannecouque, C., Van Damme, E., Peumans, W., Egberink, H., Balzarini, J., Van Ranst, M., 2007. Plant lectins are potent inhibitors of coronaviruses by interfering with two targets in the viral replication cycle. Antiv. Res. 75, 179–187 https://doi.org/10.1016/j.antiviral.2007.03.003.

Kim, D.E., Chivian, D., Baker, D., 2004. Protein structure prediction and analysis using the Robetta server. Nucleic. Acids. Res. 32, W526–W531 https://doi.org/10.1093/nar/gkh468.

Kim, P., Jang, Y., Kwon, S., Lee, C., Han, G., Seong, B., 2018. Glycosylation of Hemagglutinin and Neuraminidase of Influenza A virus as signature for ecological spillover and adaptation among influenza reservoirs. Viruses 10, 183 https://doi.org/10.3390/v10040183.

Korber, B., Fischer, W.M., Gnanakaran, S., Yoon, H., Theiler, J., Abfalterer, W., Hengartner, N., Giorgi, E.E., Bhattacharya, T., Foley, B., Hastie, K.M., Parker, M.D., Partridge, D.G., Evans, C.M., Freeman, T.M., de Silva, T.I., McDanal, C., Perez, L.G., Tang, H., Moon-Walker, A., Whelan, S.P., LaBranche, C.C., Saphire, E.O., Montefiori, D.C., Angyal, A., Brown, R.L., Carrilero, L., Green, L.R., Groves, D.C., Johnson, K.J., Keeley, A.J., Lindsey, B.B., Parsons, P.J., Raza, M., Rowland-Jones, S., Smith, N., Tucker, R.M., Wang, D., Wyles, M.D., 2020. Tracking Changes in SARS-CoV-2 Spike: evidence that D614G Increases Infectivity of the COVID-19 Virus. Cell 182, 812–827 https://doi.org/10.1016/j.cell.2020.06.043.

Kosik, I., Ince, W.L., Gentles, L.E., Oler, A.J., Kosikova, M., Angel, M., Magadán, J.G., Xie, H., Brooke, C.B., Yewdell, J.W., 2018. Influenza A virus hemagglutinin glycosylation compensates for antibody escape fitness costs. PLoS Pathogen 14, e1006796 https://doi.org/10.1371/journal.ppat.1006796.

Kumaki, Y., Wandersee, M.K., Smith, A.J., Zhou, Y., Simmons, G., Nelson, N.M., Bailey, K.W., Vest, Z.G., Li, J.K.-K., Chan, P.K.-S., Smee, D.F., Barnard, D.L., 2011. Inhibition of severe acute respiratory syndrome coronavirus replication in a lethal SARS-CoV BALB/c mouse model by stinging nettle lectin, Urticadioica agglutinin. Antiv. Res. 90, 22–32 https://doi.org/10.1016/j.antiviral.2011.02.003.

Lan, J., Ge, J., Yu, J., Shan, S., Zhou, H., Fan, S., Zhang, Q., Shi, X., Wang, Q., Zhang, L., Wang, X., 2020. Structure of the SARS-CoV-2 spike receptor-binding domain bound to the ACE2 receptor. Nature 581, 215–220 https://doi.org/10.1038/s41586-020-2180-5.

Laskowski, R.A., MacArthur, M.W., Moss, D.S., Thornton, J.M., 1993. PROCHECK: a program to check the stereochemical quality of protein structures. J. ApplCrystallogr 26, 283–291 https://doi.org/10.1107/S0021889892009944.

Lei, C., Qian, K., Li, T., Zhang, S., Fu, W., Ding, M., Hu, S., 2020. Neutralization of SARS-CoV-2 spike pseudotyped virus by recombinant ACE2-Ig. Nat. Commun. 11, 2070 https://doi.org/10.1038/s41467-020-16048-4.

Liu, Y.-M., Shahed-Al-Mahmud, Md., Chen, X., Chen, T.-H., Liao, K.-S., Lo, J.M., Wu, Y.-M., Ho, M.-C., Wu, C.-Y., Wong, C.-H., Jan, J.-T., Ma, C., 2020. A carbohydrate-binding protein from the edible lablab beans effectively blocks the infections of influenza viruses and SARS-CoV-2. Cell Rep. 32, 108016 https://doi.org/10.1016/j.celrep.2020.108016.

Mitchell, C.A., Ramessar, K., O'Keefe, B.R., 2017. Antiviral lectins: selective inhibitors of viral entry. Antiv. Res. 142, 37–54 https://doi.org/10.1016/j.antiviral.2017.03.007.

Nascimento da Silva, L.C., Mendonça, J.S.P., de Oliveira, W.F., Batista, K.L.R., Zagmignan, A., Viana, I.F.T., dos Santos Correia, M.T., 2021. Exploring lectin–glycan interactions to combat COVID-19: Lessons acquired from other enveloped viruses. Glycobiology 31, 358–371 https://doi.org/10.1093/glycob/cwaa099.

Ngo, H.X., Garneau-Tsodikova, S., 2018. What are the drugs of the future? Med. Chem. Commun. 9, 757–758 https://doi.org/10.1039/C8MD90019A.

Ooi, L.S.M., Ho, W.-S., Ngai, K.L.K., Tian, L., Chan, P.K.S., Sun, S.S.M., Ooi, V.E.C., 2010. Narcissus tazetta lectin shows strong inhibitory effects against respiratory syncytial virus, influenza A (H1N1, H3N2, H5N1) and B viruses. J. Biosci. 35, 95–103 https://doi.org/10.1007/s12038-010-0012-8.

Pascal, K.E., Coleman, C.M., Mujica, A.O., Kamat, V., Badithe, A., Fairhurst, J., Hunt, C., Strein, J., Berrebi, A., Sisk, J.M., Matthews, K.L., Babb, R., Chen, G., Lai, K.-M.V., Huang, T.T., Olson, W., Yancopoulos, G.D., Stahl, N., Frieman, M.B., Kyratsous, C.A., 2015. Pre- and postexposure efficacy of fully human antibodies against Spike protein in a novel humanized mouse model of MERS-CoV infection. Proc Natl AcadSci USA 112, 8738–8743 https://doi.org/10.1073/pnas.1510830112.

Peeples, L., 2020. News Feature: Avoiding pitfalls in the pursuit of a COVID-19 vaccine. Proc Natl AcadSci USA 117, 8218–8221 https://doi.org/10.1073/pnas.2005456117.

Ramachandraiah, G., Chandra, N.R., Surolia, A., Vijayan, M., 2002. Re-refinement using reprocessed data to improve the quality of the structure: a case study involving garlic lectin. ActaCrystallogr D BiolCrystallogr 58, 414–420 https://doi.org/10.1107/S0907444901021497.

Roy, A., Gupta, S., Hess, D., Das, K.P., Das, S., 2014. Binding of insecticidal lectin *Colocasiaesculenta* tuber agglutinin (CEA) to midgut receptors of *Bemisiatabaci* and *Lipaphiserysimi* provides clues to its insecticidal potential. Proteomics 14, 1646–1659 https://doi.org/10.1002/pmic.201300408.

Saha, P., Dasgupta, I., Das, S., 2006a. A novel approach for developing resistance in rice against phloem limited viruses by antagonizing the phloem feeding hemipteran vectors. Plant MolBiol 62, 735–752 https://doi.org/10.1007/s11103-006-9054-6.

Saha, P., Majumder, P., Dutta, I., Ray, T., Roy, S.C., Das, S., 2006b. Transgenic rice expressing Allium sativum leaf lectin with enhanced resistance against sap-sucking insect pests. Planta 223, 1329–1343 https://doi.org/10.1007/s00425-005-0182-z.

Sauerborn, M.K., Wright, L.M., Reynolds, C.D., Grossmann, J.G., Rizkallah, P.J., 1999. Insights into carbohydrate recognition by Narcissus pseudonarcissus lectin: the crystal structure at 2 Å resolution in complex with α1-3 mannobiose 1 1Edited by J. Thornton. J. Mol. Biol. 290, 185–199 https://doi.org/10.1006/jmbi.1999.2862.

Shang, J., Wan, Y., Luo, C., Ye, G., Geng, Q., Auerbach, A., Li, F., 2020. Cell entry mechanisms of SARS-CoV-2. Proc. Natl. Acad. Sci. USA 117, 11727–11734 https://doi.org/10.1073/pnas.2003138117.

Song, S.K., Moldoveanu, Z., Nguyen, H.H., Kim, E.H., Choi, K.Y., Kim, J.B., Mestecky, J., 2007. Intranasal immunization with influenza virus and Korean mistletoe lectin C (KML-C) induces heterosubtypic immunity in mice. Vaccine 25, 6359–6366 https://doi.org/10.1016/j.vaccine.2007.06.030.

Tegally, H., Wilkinson, E., Giovanetti, M., Iranzadeh, A., Fonseca, V., Giandhari, J., Doolabh, D., Pillay, S., San, E.J., Msomi, N., Mlisana, K., von Gottberg, A., Walaza, S., Allam, M., Ismail, A., Mohale, T., Glass, A.J., Engelbrecht, S., Van Zyl, G., Preiser, W., Petruccione, F., Sigal, A., Hardie, D., Marais, G., Hsiao, N., Korsman, S., Davies, M.-A., Tyers, L., Mudau, I., York, D., Maslo, C., Goedhals, D., Abrahams, S., Laguda-Akingba, O., Alisoltani-Dehkordi, A., Godzik, A., Wibmer, C.K., Sewell, B.T., Lourenço, J., Alcantara, L.C.J., Kosakovsky Pond, S.L., Weaver, S., Martin, D., Lessells, R.J., Bhiman, J.N., Williamson, C., de Oliveira, T., 2021. Detection of a SARS-CoV-2 variant of concern in South Africa. Nature 592, 438–443 https://doi.org/10.1038/s41586-021-03402-9.

Wang, C., Li, W., Drabek, D., Okba, N.M.A., van Haperen, R., Osterhaus, A.D.M.E., van Kuppeveld, F.J.M., Haagmans, B.L., Grosveld, F., Bosch, B.-J., 2020. A human monoclonal antibody blocking SARS-CoV-2 infection. Nat. Commun. 11, 2251 https://doi.org/10.1038/s41467-020-16256-y.

Weiss, S.R., Leibowitz, J.L., 2011. Coronavirus Pathogenesis. Advances in Virus Research. Elsevier, pp. 85–164 https://doi.org/10.1016/B978-0-12-385885-6.00009-2.

Xia, S., Liu, M., Wang, C., Xu, W., Lan, Q., Feng, S., Qi, F., Bao, L., Du, L., Liu, S., Qin, C., Sun, F., Shi, Z., Zhu, Y., Jiang, S., Lu, L., 2020. Inhibition of SARS-CoV-2 (previously 2019-nCoV) infection by a highly potent pan-coronavirus fusion inhibitor targeting its spike protein that harbors a high capacity to mediate membrane fusion. Cell Res. 30, 343–355 https://doi.org/10.1038/s41422-020-0305-x.

Xiang, R., Yu, Z., Wang, Y., Wang, L., Huo, S., Li, Y., Liang, R., Hao, Q., Ying, T., Gao, Y., Yu, F., Jiang, S., 2021. Recent advances in developing small-molecule inhibitors against SARS-CoV-2. Acta Pharmaceutica Sinica https://doi.org/10.1016/j.apsb.2021.06.016.

Xiu, S., Dick, A., Ju, H., Mirzaie, S., Abdi, F., Cocklin, S., Zhan, P., Liu, X., 2020. Inhibitors of SARS-CoV-2 Entry: Current and Future Opportunities. J. Med. Chem. 63, 12256–12274 https://doi.org/10.1021/acs.jmedchem.0c00502.

Xu, J., Shi, P.-Y., Li, H., Zhou, J., 2020. Broad spectrum antiviral agent niclosamide and its therapeutic potential. ACS Infect. Dis. 6, 909–915 https://doi.org/10.1021/acsinfecdis.0c00052.

Xue, L.C., Rodrigues, J.P., Kastritis, P.L., Bonvin, A.M., Vangone, A., 2016. PRODIGY: a web server for predicting the binding affinity of protein–protein complexes. Bioinformatics btw514 https://doi.org/10.1093/bioinformatics/btw514.

Yang, J., Petitjean, S.J.L., Koehler, M., Zhang, Q., Dumitru, A.C., Chen, W., Derclaye, S., Vincent, S.P., Soumillion, P., Alsteens, D., 2020. Molecular interaction and inhibition of SARS-CoV-2 binding to the ACE2 receptor. Nat. Commun. 11, 4541 https://doi.org/10.1038/s41467-020-18319-6.

Zhao, P., Praissman, J., Grant, O.C., Cai, Y., Xiao, T., Rosenbalm, K., Kellman, B., Bridger, R., Barouch, D.H., Brindley, M., Lewis, N., Tiemeyer, M., Chen, B., Woods, R., Wells, L., 2020. Virus-Receptor Interactions of Glycosylated SARS-CoV-2 Spike and Human ACE2 Receptor. Cell Host & Microbe 28 (4), 586–601. https://doi.org/10.1016/j.chom.2020.08.004.

Zhou, P., Yang, X.-L., Wang, X.-G., Hu, B., Zhang, L., Zhang, W., Si, H.-R., Zhu, Y., Li, B., Huang, C.-L., Chen, H.-D., Chen, J., Luo, Y., Guo, H., Jiang, R.-D., Liu, M.-Q., Chen, Y., Shen, X.-R., Wang, X., Zheng, X.-S., Zhao, K., Chen, Q.-J., Deng, F., Liu, L.-L., Yan, B., Zhan, F.-X., Wang, Y.-Y., Xiao, G.-F., Shi, Z.-L., 2020. Addendum: A pneumonia outbreak associated with a new coronavirus of probable bat origin. Nature 588, E6 https://doi.org/10.1038/s41586-020-2951-z.

Zhou, Y., Lu, K., Pfefferle, S., Bertram, S., Glowacka, I., Drosten, C., Pöhlmann, S., Simmons, G., 2010. A Single Asparagine-Linked Glycosylation Site of the Severe Acute Respiratory Syndrome Coronavirus Spike Glycoprotein Facilitates Inhibition by Mannose-Binding Lectin through Multiple Mechanisms. J. Virol. 84, 8753–8764 https://doi.org/10.1128/JVI.00554-10.